

Macroscopic Zeno Effect and Stationary Flows in Nonlinear Waveguides with Localized Dissipation

D. A. Zezyulin,¹ V. V. Konotop,^{1,2} G. Barontini,³ and H. Ott³

¹*Centro de Física Teórica e Computacional, Faculdade de Ciências, Universidade de Lisboa, Avenida Professor Gama Pinto 2, Lisboa 1649-003, Portugal*

²*Departamento de Física, Faculdade de Ciências, Universidade de Lisboa, Campo Grande, Ed. C8, Piso 6, Lisboa 1749-016, Portugal*

³*Department of physics and OPTIMAS research center, University of Kaiserslautern, Erwin Schrödinger Straße, 67663 Kaiserslautern, Germany*

(Received 16 December 2011; published 11 July 2012)

We theoretically demonstrate the possibility of observing the macroscopic Zeno effect for nonlinear waveguides with localized dissipation. We show the existence of stable stationary flows, which are balanced by losses in the dissipative domain. The macroscopic Zeno effect manifests itself in the nonmonotonic dependence of the stationary flow on the strength of the dissipation. In particular, we highlight the importance of the dissipation parameters in observing the phenomenon. Our results are applicable to a large variety of systems, including the condensates of atoms or quasiparticles and optical waveguides.

DOI: [10.1103/PhysRevLett.109.020405](https://doi.org/10.1103/PhysRevLett.109.020405)

PACS numbers: 03.75.Kk

Since the pioneering work of Khalfin [1] concerning the nonexponential decay of unstable atoms, the relation between the decay rate and measurement process was in the focus of many studies. One of the fundamental results of the theory, termed, after the seminal paper [2], the quantum Zeno effect, consists in slowing down the dynamics of a quantum system subjected to frequent measurements or a strong coupling to another quantum system. This phenomenon has been demonstrated in a rigorous mathematical framework in [2], and it received further refinements and extension in subsequent studies [3]. Experimentally, the quantum Zeno effect has been confirmed for single ions [4], ultracold atoms in accelerated optical lattices [5], atomic spin motion controlled by circularly polarized light [6], externally driven mixtures of two hyperfine states of neutral atoms [7], photons in a cavity [8], and the production of cold molecular gases in an optical lattice [9]. It has also been predicted [10,11] that the tunneling dynamics of particles in a double-well potential can be slowed down if the particles are removed from one of the wells. Qualitatively similar results for the suppression of atom losses in an open Bose-Hubbard chain were reported in [12]. Within the limit of an infinitely strong measurement of particles in a given spatial domain, it has been shown that the system is projected onto a unitary dynamics in the loss-free domain [13].

The Zeno effect is sometimes also understood in more general terms as the effect of changing a decay law depending on the frequency of measurements [14]. Applying this definition to a macroscopic quantum system, such as a gas of condensed bosonic atoms, and taking into account the fact that in the macroscopic dynamics the frequency of measurement can be interpreted as the strength of the induced dissipation [11], the effect of the measurement

on the decay of the quantum system can be viewed as the effect of dissipation on the macroscopic characteristics of the system. Here, we assume this interpretation of the phenomenon and address the questions on how the appearance of localized losses in a waveguide is connected to the appearance of Zeno-like dynamics. In order to emphasize the distinction of the latter statement about the problem with respect to the already standard and widely accepted notion of quantum Zeno effect, we refer, below, to the macroscopic Zeno effect (MZE), bearing in mind its mean-field manifestation.

Losses are ubiquitous for real quantum systems owing to coupling to an environment. Very often, the loss processes are also spatially localized. They can be either externally engineered (e.g., with the tip of a scanning probe microscope, a local probe in a quantum gas, an absorbing spatial domain) or intrinsically present in the form of defects and impurities. One can therefore expect that the MZE can manifest itself in a wide class of physical systems, including exciton polaritons [15], magnon gases [16], surface plasmons [17], and optics of nonlinear Kerr media [18].

We study one-dimensional nonlinear waveguides governed by the nonlinear Schrödinger equation

$$i\Psi_t = -\Psi_{xx} + g|\Psi|^2\Psi - i\gamma(x)\Psi, \quad (1)$$

where g is the nonlinearity parameter and the local loss processes are modelled by $i\gamma(x)$ (for a review on the application of complex potentials, see [19]). Since localized dissipation is applied to a homogeneous condensate (i.e., it breaks the translational invariance of the system), this can be referred to as a dissipative defect [20]. We are interested in stationary flows, which correspond to a situation when an incoming flux of particles from both ends of the waveguide is exactly balanced by the losses

in the dissipative domain. Note that in such a statement the counting of lost particles is replaced by computing the number of particles that must be loaded into the system in order to compensate the losses.

In Fig. 1, we show several examples of how such a scenario can be realized experimentally in different physical systems. While our approach is applicable to a large variety of physical situations, the systems we have in mind are those described in [20–23], i.e., an atomic Bose-Einstein condensate (BEC) subjected to removal of atoms. In this last case, the time and coordinate are respectively measured in units of $(2\omega_{\perp})^{-1}$ and $a_{\perp}/2$, where a_{\perp} and ω_{\perp} are the transverse linear oscillator length and frequency, respectively, of the transverse trap, while $g = a_s n_0$, a_s being the scattering length and n_0 the unperturbed linear density of the condensate. In what follows, we consider only the case of $g > 0$, which describes repulsive interatomic interactions (or defocusing Kerr media in optical applications).

The dissipation is described by the nonnegative localized function $\gamma(x)$, which is characterized by two control parameters, its amplitude Γ_0 and characteristic width ℓ . It is convenient to set $\gamma(x) = \Gamma_0 f(x/\ell)$, where $f(x)$ is a known smooth function such that $\max_x |f(x)| = f(0) \sim 1$ and $\max_x |f_x(x)| \sim 1$. Then, Γ_0 and ℓ are proportional to the intensity of the defect: $\int_{-\infty}^{\infty} \gamma(x) dx \propto \Gamma_0 \ell$. We will also assume the most typical experimental situation where $\gamma(x)$ is an even function, $\gamma(x) = \gamma(-x)$, with only one maximum at $x = 0$. Keeping in mind the experiments of Refs. [21–23], one can estimate $\Gamma_0 \sim I\sigma_{\text{ion}}/(e_0\omega_{\perp})$, where I is the current of the electron beam, e_0 the electric charge of the electron, and σ_{ion} the total ionization cross section.

Stationary flows are sought in the form $\Psi_{st}(t, x) = \rho(x) \exp[i \int_0^x v(s) ds - i\mu t]$, where $v(x)$ is the superfluid

velocity, μ the chemical potential, and $\rho^2(x) = n(x)$ the density. Substituting $\Psi_{st}(t, x)$ into Eq. (1), we obtain

$$\rho_{xx} + \mu\rho - g\rho^3 - j^2\rho^{-3} = 0, \quad j_x + \gamma(x)\rho^2 = 0 \quad (2)$$

where $j(x) = v(x)n(x)$ is the superfluid current. We are interested in the solution of Eq. (2) with a constant density at infinity, $\lim_{|x| \rightarrow \infty} |\rho(x)| = \rho_{\infty}$. Then, $\mu = j_{\infty}^2 \rho_{\infty}^{-4} + g\rho_{\infty}^2$, where $j_{\infty} = \mp \lim_{x \rightarrow \pm\infty} j(x)$ is a positive constant. For any stationary flow, the loss of particles in the defect has to be balanced by the incoming current j_{∞} . The main objective of the present study is to show the existence of such stationary flows and explore the dependence of the current j_{∞} on the parameters of the defect.

First, we consider an example that allows for an exact solution, extending the result of [20]. We assume a dissipative defect of the particular form $\gamma(x) = 3\Gamma_0 \text{sech}^2(x/\ell)$. Then, it is straightforward to show that $\rho(x) = \tanh(x/\ell)$ and $j(x) = -\Gamma_0 \ell \tanh^3(x/\ell)$ are solutions of the system (2) provided that $\ell^2(g + \Gamma_0^2 \ell^2) = 2$. Thus, the incoming flux is linearly proportional to the intensity of the dissipative defect $j_{\infty} = \Gamma_0 \ell$, and in order to obtain a stationary solution, any increase in the strength of the dissipation must be compensated with an increase in the incoming flux. In other words, if the incoming flux of particles is increased, the excess particles can be removed only by a stronger defect. While this result is quite intuitive, we show below that it does not hold in general. In particular, we will show that for appropriate parameters, an increasing flux can be compensated by a weaker defect.

We now focus on a dissipation with finite support, $\gamma(x) \equiv 0$ if $|x| > \ell$. This form of the dissipative term models, in particular, the electronic beam used in [21,22]. In order to decrease numerical errors, we choose $\gamma(x)$ to be smooth at the edges of the dissipative domain, $\gamma(x) = \Gamma_0(1 - x^2/\ell^2)^2$ if $|x| < \ell$.

Since Eq. (2) is not integrable, unlike its conservative counterpart where $\gamma(x) \equiv 0$, it is convenient to treat Γ_0 as a parameter that increases, departing from zero. Experimentally, this would correspond to an adiabatic increase of the defect intensity. For $\Gamma_0 = 0$, one recovers two well-known solutions: a constant density $\rho(x) = \rho_{\infty}$ and a dark soliton $\rho(x) = \rho_{\infty} \tanh(\sqrt{g/2}\rho_{\infty}x)$ [$j(x) \equiv 0$] for both solutions. When the defect is adiabatically switched on, the constant density and dark soliton originate two branches of solutions. The branch bifurcating from the constant density consists of symmetric flows, for which the relation $\rho(x) = \rho(-x)$ holds. The flows that branch off from the dark soliton are antisymmetric, $\rho(x) = -\rho(-x)$. From the second part of Eq. (2) it follows that both the symmetric and antisymmetric flows possess odd currents, $j(x) = -j(-x)$.

Considering the behavior of the solutions in the vicinity of $x = 0$, for the symmetric flows we obtain $\rho_{xx}(0) = \rho(0)[g(\rho^2(0) - \rho_{\infty}^2) - j_{\infty}^2 \rho_{\infty}^{-4}]$. Thus, employing a physically obvious condition $\rho_{\infty} > \rho(0) > 0$, we find that

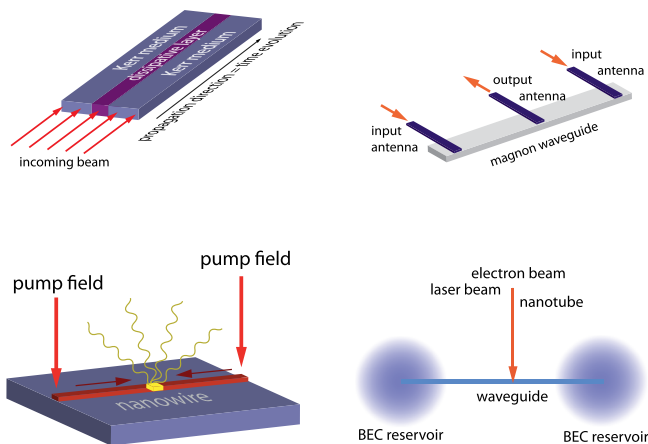


FIG. 1 (color online). Possible experimental scenarios to observe the MZE: nonlinear optical waveguide (upper left), a magnon waveguide (upper right), a plasmonic nanostructure (lower left), an atomic BEC in a waveguide, and two reservoirs (lower right).

$\rho_{xx}(0) < 0$. We therefore arrive at the counterintuitive conclusion that for symmetric flows the atomic density $n(x)$ has a local maximum at the point of maximal dissipation.

On the other hand, for $x \rightarrow \infty$, both symmetric and antisymmetric flows behave as

$$\rho_\infty - \rho(x) \propto e^{-\sqrt{\Lambda}x}, \quad \text{where } \Lambda = 2g\rho_\infty^2 - 4j_\infty^2\rho_\infty^{-4}. \quad (3)$$

Thus, for a given density ρ_∞ , there exists an upper bound for the maximal current $j_\infty^{\max} = \sqrt{g\rho_\infty^3}/\sqrt{2}$ above which no stationary flow can exist.

In Fig. 2(a) [Fig. 2(b)], we show the density profiles $n(x)$ of symmetric (antisymmetric) flows for different values of the dissipation strength Γ_0 . We observe that for the symmetric flows, the density possesses two deep local minima. For a weak dissipation (e.g., $\Gamma_0 = 0.01$), the minima are situated outside the dissipative domain, which allows us to compute the exact value of the density in these minima: $n_{\min} = 2j_\infty^2\rho_\infty^{-4}/g$. As the strength of the dissipation grows, the minima move from $\pm\infty$ toward the center and eventually enter the dissipative domain. For antisymmetric flows, the dependence of the density on Γ_0 is much weaker pronounced [the curves for different Γ_0 are hardly distinguishable on the scale of Fig. 2(b)].

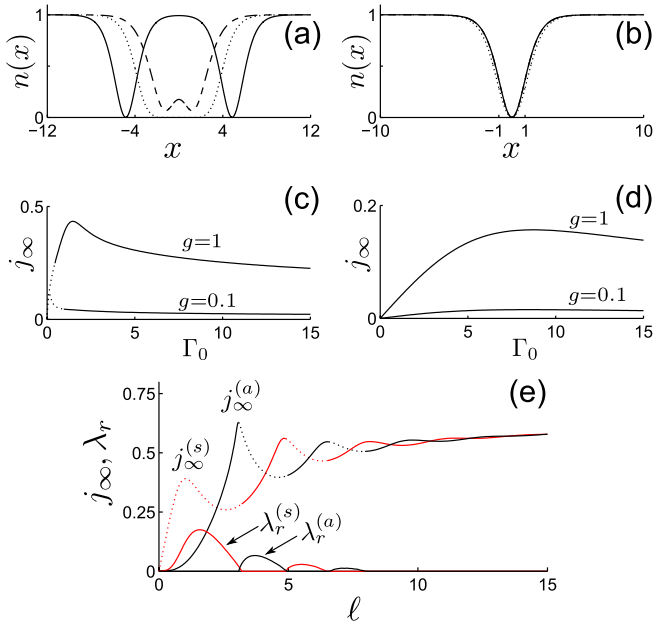


FIG. 2 (color online). (a) Density distributions $n(x)$ for symmetric flows for $g = 1$ and $\ell = 4$ and different values of Γ_0 . Solid line: $\Gamma_0 = 0.01$; dashed line: $\Gamma_0 = 1$; dotted line: $\Gamma_0 = 10$. (b) Density distributions $n(x)$ for antisymmetric flows for $g = 1$ and $\ell = 1$. Solid line: $\Gamma_0 = 0.1$; dashed line: $\Gamma_0 = 1$; dotted line: $\Gamma_0 = 10$. (c) and (d) Current vs strength of the dissipation for symmetric flows (with $\ell = 4$) and antisymmetric flows (with $\ell = 1$) obtained for $g = 0.1$ and $g = 1$; stable (unstable) flows correspond to the solid (dotted) fragments of the curves. (e) Currents and instability increments vs width of the defect for symmetric [(s)] and antisymmetric [(a)] flows for $g = 1$ and $\Gamma_0 = 1$. In all panels, $\rho_\infty = 1$.

Now our goal is to study the dependence j_∞ vs Γ_0 . The typical results for symmetric (antisymmetric) flows are illustrated in Fig. 2(c) [Fig. 2(d)]. When nonlinearity is sufficiently strong ($g = 1$), for both types of flows one can clearly see a global maximum of $j_\infty(\Gamma_0)$. When Γ_0 exceeds the value corresponding to this maximum, the required current j_∞ decreases. This is the manifestation of the MZE.

In order to observe the MZE in an experiment, it is important that the solutions be stable. To examine the stability of the flows, we substitute $\Psi(t, x) = \Psi_{st}(t, x) + e^{-i\mu t}[a_+(x)e^{\lambda t} + a_-(x)e^{\lambda^* t}]$ into Eq. (1), linearize it with respect to $a_\pm(x)$, and solve the obtained linear eigenvalue problem. Instability occurs if there exists an eigenvalue λ with a positive real part λ_r . The analysis results are shown in Figs. 2(c)–2(e). For the symmetric flows presented in Fig. 2(c), small values of Γ_0 do not allow for stable stationary flows (see the dotted fragments of the lines). For instance, the symmetric flow with two local minima situated outside of the dissipative domain [shown in Fig. 2(a) and corresponding to $\Gamma_0 = 0.01$] is unstable. For larger values of Γ_0 , the symmetric flows become stable. We have observed that the two minima of a stable symmetric flow are always located in the dissipative domain. All antisymmetric flows shown in Fig. 2(d) are stable. Most importantly, the parameter range in which the MZE is observed has only stable flows. From an experimental point of view, the existence of stable symmetric flows is very appealing, as symmetric flows arise from the overall (symmetric) ground state of the system.

We now elaborate on the role of the size of the defect. In Fig. 2(e), we show the currents vs ℓ for a fixed Γ_0 . As the defect becomes wider, one might expect a monotonic increase of j_∞ . As can be seen from the graph, this behavior is indeed encountered, however, only on average. Locally, it is superimposed by a resonance-like structure that tends to enhance the current for certain defect sizes. We also find that stable solutions appear only when $j_\infty(\ell)$ is a growing function and (up to a certain degree of accuracy) the domains of stability of the symmetric flows coincide with the domains of instability of the antisymmetric flows, and vice versa.

So far, we have encountered two different situations: in the case of the sech^2 -shaped dissipation, the branch of stationary flows does not show the MZE; in the case of the dissipation with finite support, the MZE has various manifestations. The difference can be explained by examining the asymptotic behavior of the corresponding flows. In the case of the sech^2 -shaped dissipation, the asymptotic behavior at $x \rightarrow \infty$ of the density is completely determined by the characteristic width ℓ of the defect $\rho_\infty - \rho(x) \sim 2e^{-2x/\ell}$, while the flows supported by the dissipation with finite support behave according to Eq. (3). Moreover, Eq. (3) implies that there exists the maximal possible current j_∞^{\max} . It appears that the presence of such a threshold is a signature of the MZE. No such threshold exists for the stationary flows with the

sech²-shaped dissipation: the current, j_∞ , can be arbitrarily large, and the MZE is not found.

However, the sech²-shaped dissipation still does not forbid the MZE in principle, since flows obeying Eq. (3) can also be found in this case. Let us revisit the dissipation of the form $\gamma(x) = 3\Gamma_0 \text{sech}^2(x/\ell)$. Substituting $\rho(x) = \rho_\infty - \rho_1(x)$ [where $\rho_1(x) = o(1)$ as $x \rightarrow \infty$] into Eq. (2) and neglecting the terms of smaller order, one observes that for $x \gg 1$, function $\rho_1(x)$ is described by the equation $\rho_{1,xx} - \Lambda\rho_1 = 12j_\infty\Gamma_0\ell\rho_\infty^{-1}e^{-2x/\ell}$. For $\rho_1(x)$ to obey the asymptotics (3), the following two conditions must be fulfilled: (i) $\Lambda > 0$ —gives the maximal current $j_\infty < j_\infty^{\max}$; (ii) $\sqrt{\Lambda} < 2/\ell$ —yields the minimal possible current $j_\infty > j_\infty^{\min} = \rho_\infty\sqrt{g\rho_\infty^4/2 - \ell^{-2}}$ (if the expression under the radical is negative, then $j_\infty^{\min} = 0$). As ℓ grows, j_∞^{\min} approaches j_∞^{\max} . Hence, the range of currents allowing the solutions that obey Eq. (3) decreases. This leads us to the conjecture that rapidly decaying dissipation is favorable for the observation of the MZE. In particular, the defects decaying faster than exponentially are more likely to display the MZE than the ones obeying exponential decaying.

We close this Letter with a discussion on the possible experimental observation of the obtained MZE. The incoming flux of particles has to be generated at both ends of the waveguide. This can be achieved by controlled pumping terms in the case of quasiparticles, or by reservoirs in the case of real particles. For light propagating in a nonlinear waveguide, such boundary conditions appear rather naturally. But even for a finite system with no reservoir, one can speculate that a quasistationary state is established on intermediate time scales in a transient regime; if the defect is switched on in a finite system that is initially in its ground state, the stationary flow will develop out of the symmetric initial conditions and retain its symmetry with increasing dissipation. With time, a flow of particles toward the defect is created, which mimics the boundary conditions, applied in the preceding discussion. The condition of having a defect that drops faster than exponentially can be easily realized in most of the experimental implementations suggested above.

We now support this reasoning by illustrating the generation of stationary flows through direct integration of Eq. (1) on a finite domain subject to the boundary conditions $\Psi(t, \pm L) = \rho_\infty e^{-i\mu t}$ (here L is the half-width of the computational domain). In Fig. 3, we show the temporal evolution of the atomic density for three different widths of the defect. For all the shown evolutions, the initial density is taken to be constant, and the chosen boundary conditions fix the density and chemical potential at the edges of the computational domain. Figure 3(a) shows the evolution for a set of parameters, where a stable symmetric stationary flow exists. After an initial decrease in the density at the location of the defect, the system achieves the stationary flow. In the vicinity of the origin, one clearly observes the two local minima residing inside

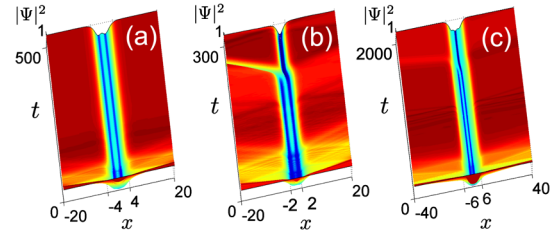


FIG. 3 (color online). Evolution of the density $|\Psi(t, x)|^2$ starting from the initial data $\Psi(0, x) = 1$. For all the shown panels, $\rho_\infty = g = \Gamma_0 = 1$. (a) The width of the defect is $\ell = 4$. The generation of the symmetric stationary flow occurs. (b) and (c) The width of the defect is $\ell = 2$ and $\ell = 6$. The symmetric flows are unstable, and therefore no stationary flow is established.

the defect. Indeed, the density eventually approaches the stationary flow profile not only in the vicinity of the origin but also in the entire computational domain. However, if the symmetric flow is not expected to be stable [Figs. 3(b) and 3(c)], the density profile would show ongoing distortions in the vicinity of the origin and eventually lose its symmetry. For the cases shown in panels (b) and (c), the density tends to approach a profile corresponding to a stable antisymmetric flow that exists for the chosen values of ℓ and Γ_0 [recall that the domains of the stability of the symmetric and antisymmetric flows alternate as shown in Fig. 2(e)]. However, in the cases (b) and (c), truly stationary antisymmetric flows are not established because the chosen boundary conditions can support only symmetric flows, which are unstable for the chosen parameters.

In summary, we have analyzed a nonlinear waveguide with a localized dissipative defect. We found evidence for the appearance of the MZE for specific boundary conditions and analyzed the role of the interaction and the defect size. The observed MZE is intrinsically related to the existence of the stable stationary flows and expressed through nonmonotonic dependence of the intensity of the dissipation on the density of incoming currents. The proved existence of stable solutions for symmetric flows is very important, as these solutions correspond to many natural experimental situations.

The collaborative study was supported by a bilateral program between DAAD (Germany) and FCT (Portugal). We acknowledge financial support by the DFG within the SFB/TRR 49 and FCT through Grant PESt-OE/FIS/UI0618/2011. D. A. Z. is supported by FCT under Grant No. SFRH/BPD/64835/2009. G. B. is supported by a Marie Curie Intra-European Fellowship.

- [1] L. A. Khal'fin, Dokl. Akad. Nauk SSSR **115**, 277 (1957); [Sov. Phys. Dokl. **2**, 232 (1958)]; Zh. Eksp. Teor. Fiz. **33**, 1371 (1958); [Sov. Phys. JETP **6**, 1053 (1958)].
- [2] B. Misra and E. C. G. Sudarshan, *J. Math. Phys. Sci.* **18**, 756 (1977).

- [3] A. G. Kofman and G. Kurizki, *Nature (London)* **405**, 546 (2000); *Phys. Rev. Lett.* **87**, 270405 (2001); P. Facchi and S. Pascazio, *ibid.* **89**, 080401 (2002); A. Barone, G. Kurizki, and A. G. Kofman, *ibid.* **92**, 200403 (2004); I. E. Mazets, G. Kurizki, N. Katz, and N. Davidson, *ibid.* **94**, 190403 (2005).
- [4] W. M. Itano, D. J. Heinzen, J. J. Bollinger, and D. J. Wineland, *Phys. Rev. A* **41**, 2295 (1990).
- [5] M. C. Fischer, B. Gutiérrez-Medina, and M. G. Raizen, *Phys. Rev. Lett.* **87**, 040402 (2001).
- [6] T. Nakanishi, K. Yamane, and M. Kitano, *Phys. Rev. A* **65**, 013404 (2001).
- [7] E. W. Streed, J. Mun, M. Boyd, G. K. Campbell, P. Medley, W. Ketterle, and D. E. Pritchard, *Phys. Rev. Lett.* **97**, 260402 (2006).
- [8] J. Bernu, S. Deléglise, C. Sayrin, S. Kuhr, I. Dotsenko, M. Brune, J. M. Raimond, and S. Haroche, *Phys. Rev. Lett.* **101**, 180402 (2008).
- [9] N. Syassen, D. M. Bauer, M. Lettner, T. Volz, D. Dietze, J. J. García-Ripoll, J. I. Cirac, G. Rempe, and S. Dürr, *Science* **320**, 1329 (2008).
- [10] J. I. Cirac, A. Schenzle, and P. Zoller, *Europhys. Lett.* **27**, 123 (1994).
- [11] V. S. Shchesnovich and V. V. Konotop, *Phys. Rev. A* **81**, 053611 (2010).
- [12] D. Witthaut, F. Trimborn, H. Hennig, G. Kordas, T. Geisel, and S. Wimberger, *Phys. Rev. A* **83**, 063608 (2011); P. Barmettler and C. Kollath, *Phys. Rev. A* **84**, 041606 (2011).
- [13] P. Facchi and S. Pascazio, *J. Phys. A* **41**, 493001 (2008).
- [14] L. A. Khalifin, *Usp. Fiz. Nauk* **160**, 185 (1990); [*Sov. Phys. Usp.* **33**, 868 (1990)].
- [15] A. Amo *et al.*, *Nature (London)* **457**, 291 (2009); A. Amo, T. C. H. Liew, C. Adrados, R. Houdré, E. Giacobino, A. V. Kavokin, and A. Bramati, *Nature Photon.* **4**, 361 (2010).
- [16] S. O. Demokritov, V. E. Demidov, O. Dzyapko, G. A. Melkov, A. A. Serga, B. Hillebrands, and A. N. Slavin, *Nature (London)* **443**, 430 (2006); S. Schäfer, V. Kegel, A. A. Serga, B. Hillebrands, and M. P. Kostylev, *Phys. Rev. B* **83**, 184407 (2011).
- [17] M. Aeschlimann, T. Brixner, A. Fischer, C. Kramer, P. Melchior, W. Pfeiffer, C. Schneider, C. Strüber, P. Tuchscherer, and D. V. Voronine, *Science* **333**, 1723 (2011); Z. Ma, X. Zhang, X. Guo, Q. Yang, Y. Ma, and L. Tong, *Appl. Phys. Lett.* **96**, 051119 (2010).
- [18] F. Kh. Abdullaev, V. V. Konotop, and V. S. Shchesnovich, *Phys. Rev. A* **83**, 043811 (2011); F. Kh. Abdullaev, V. V. Konotop, M. Ögren, and M. P. Sørensen, *Opt. Lett.* **36**, 4566 (2011).
- [19] J. G. Muga, J. P. Palao, B. Navarro, and I. L. Egusquiza, *Phys. Rep.* **395**, 357 (2004).
- [20] V. A. Brazhnyi, V. V. Konotop, V. M. Pérez-García, and H. Ott, *Phys. Rev. Lett.* **102**, 144101 (2009).
- [21] T. Gericke, C. Utfeld, N. Hommerstad, and H. Ott, *Laser Phys. Lett.* **3**, 415 (2006).
- [22] T. Gericke, P. Würtz, D. Reitz, T. Langen, and H. Ott, *Nature Phys.* **4**, 949 (2008).
- [23] V. Guarrera, P. Würtz, A. Ewerbeck, A. Vogler, G. Barontini, and H. Ott, *Phys. Rev. Lett.* **107**, 160403 (2011).